Analysis of the influence of outdoor surface heat flux on the inlet water and the exhaust air temperature of the wetting pad of a direct evaporative cooling system

Ndukwu M. C.[a*], Leonard Akuwueke[a], Ugwu Elijah[a], Abam. F.I[b]., Hongwei Wu[c], Jude Mbanasor[d]
[a]Department of Agricultural and Bio-Resources Engineering, Michael Okpara University of Agriculture Umudike, P.M.B.7267, Umuahia, Nigeria;
[b]Energy, Exergy and Environment Research Group (EEERG), Department of Mechanical Engineering, Michael Okpara University of Agriculture Umudike, P.M.B.7267, Umuahia, Nigeria;
[c]School of Physics, Engineering and Computer science, University of Hertfordshire, Hatfield, AL10 9AB, UK

[d]Department of Agribusiness, Michael Okpara University of Agriculture Umudike, P.M.B.7267, Umuahia, Nigeria

*Email: ndukwumcu@gmail.com or ndukwumcu@mouau.edu.ng

Abstract

The study investigates the interconnectivity between the inlet water temperature, wind flow rate, and storage water heat flux with the performance of the wetting pads in direct evaporative cooling systems using theoretical heat and mass transfer and experimental analysis under the external ambient condition of West sub-Saharan Africa. Thus, a standalone direct, evaporative cooling system with an upper water storage tank exposed to wind flow was locally developed and evaluated with jut, palm fruit mesocarp and wood charcoal as biomass cooling pad at three air velocities. The results indicated that increasing the heat flux around the water tank and decreasing the relative humidity of the inlet air through the wetting pad will lower both the inlet water and pad exhaust temperatures. The water demand was higher in palm fruit mesocarp fibre at airflow rates of 3 m/s, while at 4 and 4.5 m/s, it was higher in wood charcoal, and the value ranged from 9.64×10^{-4} to 1.46×10^{-3} kg/s. With the exception of jute fibre at 4 m/s, higher humidity difference or low cold room temperature did not translate to higher evaporative cooling effectiveness or efficiency. However, the lower inlet water temperature significantly affected the evaporative effectiveness. This shows the possibility of free moisture transfer into the cold room from the pad materials at increased air flow rates that helped boost the exhaust air's humidity. The average evaporative efficiency for the three pads ranged from 56.4 % to 80.96 %. The values for the enlargement coefficient ranged from 5 to 6.82, while the temperature thermal stress ranged from 24.37 to 28.66 ^{o}C.

Key words: Biomass pad; DEC; Fruits and Vegetables; Passive cooling; Storage

Nomenclature

			Greek letters
A	Humidifier surface area (m^2)	ε	The emissivity of the storage tank surface (Wm^{-2})
C_p	Specific heat capacity (J/kg k)	λ	Thermal conductivity (W/m·K)
d	Thickness of the humidifier (m)	ω	Specific humidity (kg/kg)
h_c or h_{cm}	Heat transfer coefficient (W/m^2 k)	$\dot{m}$	The mass flow rate (kg/s)
h_m	Mass transfer coefficient (m/s)	ρ	Density ($kg\ m^{-3}$)
L	Latent heat of the vaporization of water(J/kg k)		
m	Mass (kg)		Subscripts
p	Pressure (Pa)	i or 1	Inlet
r	The relative amount of water absorbed (kg)	a	Ambient or air
Rh	Relative humidity (%)	e	Evaporated water
T	Temperature (°C) or K	wb	Wet bulb
W	Moisture content (-)	db	Dry bulb
		e	Effective
		atm	Atmosphere
		v	Vapour
		d	Dry
		w	Water or wind
		f or H	Humidifier
		c	Critical value
		ws	Water at saturation
		Hs	Saturated humidifier
		s	Saturation
		out or o or 2	outlet

1. Introduction

The increasing global demand for environmentally friendly energy systems has led researchers to seek alternative refrigeration systems to preserve agricultural produce. For long, evaporative cooling systems (EVC) has been used by different civilizations for home cooling, cooling or preservation of fruits and vegetables, livestock house temperature regulation etc. [1,2]. The main components of EVC are the cooling pads, which are loaded into a pad holder, the fan, the water distribution network, the pump and the cold room or storage space where the cold air is discharged into. The schematic of a typical EVC system showing the components is presented in Figure 1. The two most common designs of EVC are the direct evaporative cooling system and the indirect evaporative cooling system. In direct evaporative cooling (DEC) design, the ambient air is supplied directly to the cooling pad without dehumidification [3]. In contrast, the indirect evaporative cooling (IEC) system is equipped with a secondary heat exchanger that prevents the humidity from the primary air supply from rising in the air stream that discharges into the cooled space [4]. The technology of IEC is mostly used in homes and livestock buildings due to the ability to supply cooled air at lower temperatures and prevent humidity rise of the primary air compared to DEC [4, 5].

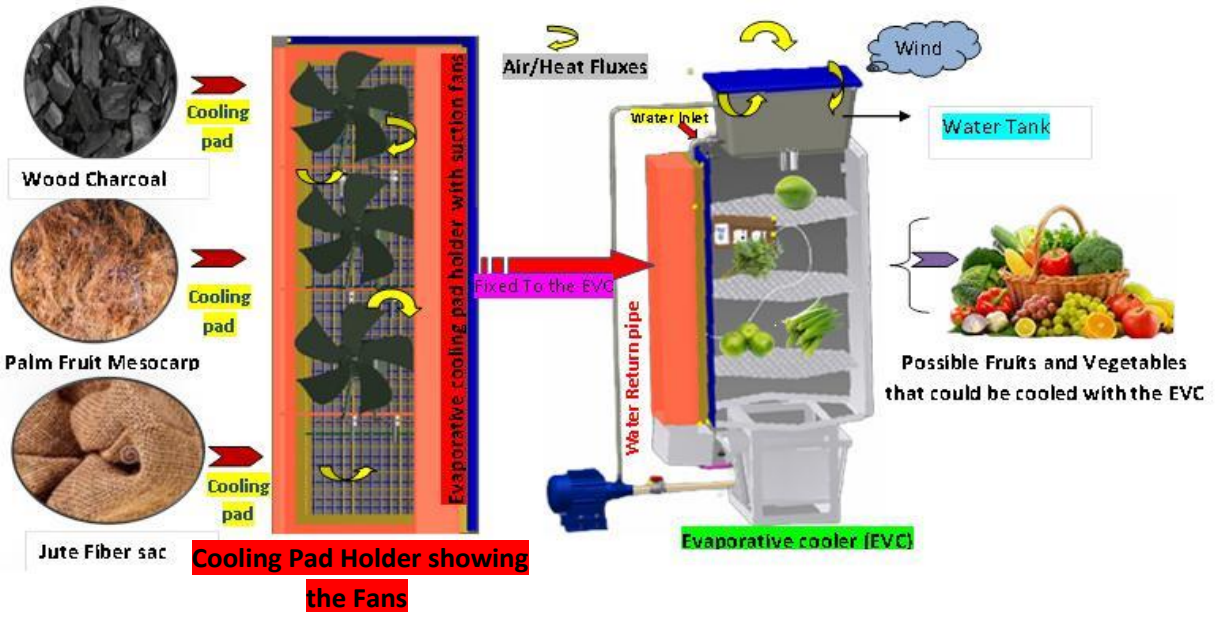

Figure 1: Graphic depiction of the cooling pad materials, loading in the pad holder and loading the vegetables

Nevertheless, DEC is the most adopted design in low-income countries due to its simplicity and the low cost of fabrication [6]. Additionally, due to its high indoor relative humidity and the simplicity of design, the DEC design has been deployed in the cooling and storage of agricultural products by several studies [7,8]. This is because to maintain the freshness of fruits and vegetables and, retain their quality, they require lower temperatures and high humidity [9]. Therefore several studies are available on using evaporative cooling systems to store fruits and vegetables with different kinds of materials as a cooling pad. For example, the storage life of leafy amaranths was extended to 8 days using EVC with wet sand as cooling pads [10]. The study showed that the amaranths lost only 16.9% of their weight on the eighth day. Similarly, Islam and Morimoto [11], achieved a storage life of 19 for egg plants with sand and zeolite as a cooling pad. Additionally, Ndukwu et al [12] achieved a storage life of 19 days for tomatoes in a tropical climate using clay type evaporative cooler while Dalchi et al [13] extended the shelf life of several fruits and vegetables that includes tomatoes, carrot peas, spinach, green onions, etc., to 3-5 days using EVC with sand as a cooling pad. Furthermore, several biomass materials have also been used as cooling pads in EVC. These materials made from agricultural residues are found to be good and cheaper substitutes to expensive and non-biodegradable industrial manufactured pads like Aspen, CELDEK etc. Moreover, these materials are available at lower or no cost depending on the treatments given to them before use and even if they require to be changed regularly, it might not drastically add to the cost of the EVC because some of them are mostly obtained at no cost [6]. Thus, some biomass materials that have been used in literature include coconut coir [14, 15], coconut and Palash fibres [16], rice by-products, bamboo chips, palm fibre, wood fibres etc [17]. Eucalyptus fibres [18], Luffa pad Aziz et al [19], Khus, [20], Rice straw [21]. However, a review of the literature by Ndukwu and Manuwa [6], showed that studies on the use of new biomass materials as cooling pads in EVC are still ongoing in different regions of the world. The aim is to provide low-cost materials for EVC design to make it affordable in these regions. Therefore the

performance of these biomass materials needs to be studied both experimentally and theoretically using a functional evaporative cooler of different kinds of design to generate data for its practical application and replication in different regions.

Generally from the above literature studies, the focus of most research has been on the number of days the DEC can store the product only but they lack the serious theoretical analysis that can assist in the optimization of the various developed systems. According to Tejero-Gonzalez and Franco-Salas [22], the dynamics of the heat flux around the water tank and cooling pad in passive evaporative cooling is less focused on. However, It has been postulated that in direct evaporative cooling systems, the process is adiabatic; therefore, the temperature of water re-circulated through the cooling pads and the inlet air is at the same wet bulb temperature of the inlet air [4,22, 23]. Hence, some researchers have given a different result by recording the water temperature below or above the dry bulb temperature of the inlet air [24-27]. The critical factor observed that affects this variation is the ambient wind speed changes powered by the solar flux for different areas [28]. This is because in DEC design the air supply flux to the pads and water recirculation can be by natural convection which is influenced by the ambient wind or it can be driven by blowers or fans [29]. Therefore, Alamdari et al. [30] concluded that the performance of outdoor installed standalone DEC might not be adiabatic due to the effect of wind and solar radiation. Often researchers overlook this aspect of analysis in evaporative cooling studies. The general belief is that the humidity of the incoming air passing through the cooling pad and the pad thickness is a significant determinants of the indoor cooler temperature in DEC [31]. Still, the temperature of mixing water with the air might be an essential factor, too, especially in fresh fruits and vegetable preservation, where high indoor humidity and lower indoor temperature are required. It's of interest to note that, though the atomized water spray on the cooling pad is cooled by the heat exchange between the incoming air and the sprayed moisture in DEC but the temperature of the incoming water from the water storage tank for a standalone DEC is passively cooled and therefore influenced by air flux surrounding the tank. The ambient wind speed drives the dynamics of the heat flux around the water tank and cooling pad in passive evaporative cooling. A review of the literature by Tejero-Gonzalez and Franco-Salas [22] has revealed this aspect as the less-studied performance index for DECs. Nevertheless, many authors present data on solar radiations but not on heat flux, and they hardly corroborate this data with the overall performance of the DEC with different biomass pads. This informed the objective of this study. Therefore, this study aims to determine the influence of heat flux on the storage water temperature and the overall outlet temperature of palm fruit fibres, wood charcoal and jute fibre as biomass cooling pads in direct evaporative cooling systems.

2. Research approach and Theoretical analysis

2.1 Determination of heat flux on the storage Tank

The total heat flux (or heat transfer rate) is often used to represent the cooling capacity of the surface subject to evaporative cooling. However, it is assumed that it is passively evaporative cooled to deduce the heat flux around the storage water tank. At the same time, the humidifiers are actively evaporative cooled with the help of a fan. The total heat flux around the surface of the water storage tank consists of radiative heat exchange with the surroundings, the sensible and the latent heat fluxes are given as follows [32]

$$\dot{Q}_{tot} = \dot{Q}_l + \dot{Q}_s + \Delta\dot{Q}_r \qquad 1$$

$$\dot{Q}_l = \frac{\mathrm{h_c}}{Le^{2/3} C_{p,a}} L(\omega_w - \omega_a) \quad (2a)$$

Where the evaporative flux formed part of latent heat flux and is given equally to the mass flow rate of water evaporated as follows

$$\frac{\mathrm{h_c}}{Le^{2/3} C_{p,a}} (\omega_w - \omega_a) = \dot{m}_{ev} \quad (2b)$$

Le is the Lewis number taken as 0.865 [33, 34]

$$\dot{Q}_s = \mathrm{h_c}(T_a - T_w) \quad (3)$$

$$\Delta\dot{Q}_r = \varepsilon \times 5.67 \times 10^{-8} \times \Delta T^4 \quad (4)$$

Furthermore, to determine the heat transfer coefficient of a passively cooled surface wholly exposed to wind, it is assumed that wind speed is the only influential parameter [32]. Therefore a linear parametric equation linking the wind speed with the heat transfer coefficient is used as follows

$$\mathrm{h_c} = 5.56 + 3.62\, u_w \quad (5)$$

The specific humidity (ω) is deduced as follows [35]

$$\omega = \frac{\epsilon.\mathrm{P_v}}{P_{atm} - P_{v.}(1-\epsilon)} \quad (6)$$

Where P_{atm} is given as 101325 Pa, ϵ is the gas constant ratio between wet air and dry air given as 0.622 kg kg^{-1}, and P_v is the vapour pressure (Pa) calculated as follows [3]

$$\mathrm{P_v} = 610.8\, exp\left(\frac{17.27\, T}{T+273}\right) \quad (7)$$

2.2 Determination of heat flux on the wetting pad

The heat flux around the wetting (cooling pad or humidifier) pad consists of the conductive sensible and latent heat fluxes respectively as shown.

$$Q_H = Q_{Hc} + Q_{Hs} + Q_{Hl} \quad (8)$$

The conductive heat flux on the humidifiers was deduced with the assumption that as the material absorbs moisture; its thermal conductivity approaches the thermal conductivity of water. Therefore, the heat flux is theoretically given for one-dimensional heat flow as follows [36]

$$Q_{Hc} = -\lambda_e A \frac{\Delta T}{d} \quad (9)$$

Where ΔT is the change in temperature, while the effective thermal conductivity of the wetted material is given as follows [36]

$$\lambda_e = \lambda_f + r\frac{\lambda_w - \lambda_f}{r_c} \quad (10)$$

$$r = \frac{\mathrm{m_w}}{\mathrm{m_H}} \quad (11)$$

$$\mathrm{m_w} = (\omega_c - \omega_a)\dot{m}_a \quad (12)$$

$$r_c = \frac{\mathrm{m_{ws}}}{\mathrm{m_H}} \quad (13)$$

$$\mathrm{m_{ws}} = \mathrm{m_{Hs}} - \mathrm{m_H} \quad (14)$$

$$\mathrm{m_{Hs}} = \frac{\mathrm{m_H}}{1-\mathrm{W_s}} \quad (15)$$

At saturation, the saturated outlet air and the humidifier are at the same moisture content. Therefore the moisture content at saturation is determined as follows [4]

$$\mathrm{W_s} = 0.622\frac{\mathrm{p_s}}{\mathrm{p_a}-\mathrm{p_s}} \quad (16)$$

Where pa is given as 101325 Pa, p_s is the saturated water vapour partial pressure (Pa) deduced empirically as follows [4]

$$ln(\mathrm{p_s}) = \frac{b_1}{T_w} + b_2 + b_3 T_w + b_4 T_w^2 + b_5 T_w^3 + b_6(lnT_w) \quad (17)$$

Where b_1, b_2, b_3, b_4, b_5 and b_6 were coefficients given by Yang et al.[4] as - 5800.2206, 1.3914993, - 0.048640239, 0.41764768×10^{-4}, $-0.14452093\times 10^{-7}$ and 0, respectively. The wet bulb temperature is deduced with equation 16 as follows [37]

$$\mathrm{T_w} = T_{db} \times \arctan\left[0.151977 \times \sqrt{R\mathrm{h} + 8.313659}\right] + \arctan(T_{db} + R\mathrm{h}) - \arctan(R\mathrm{h} - 1.67633) + 0.00391838 \times (R\mathrm{h})^{3/2} \times \arctan(0.023101 \times R\mathrm{h}) - 4.686035 \quad (18)$$

The sensible heat flux is given as follows

$$Q_{Hs} = \mathrm{h_m}(\mathrm{T_a} - \mathrm{T_{out}}) \quad (19)$$

The mass transfer coefficient deduced according to Franco et al [38] as follows

$$\mathrm{h_m} = \frac{\mathrm{m_e}}{\mathrm{A_H}\Delta\rho_\mathrm{v}} \quad (20)$$

The evaporated water is given as follows [39]

$$\mathrm{m_e} = (\omega_i - \omega_o)\dot{m}_a \quad (21)$$

The specific humidity of the air inlet and the outlet air from the humidifier is deduced with equations 6 and 7 respectively. In contrast, T in equation 7 is substituted with an outlet temperature of the humidifier. The change in the density of water $\Delta\rho_v$ is determined as follows

$$\Delta\rho_v = \frac{\rho_{v2}-\rho_{v1}}{\ln(\rho_{v1}-\rho_{vwb}/\rho_{v2}-\rho_{vwb})} \quad (22)$$

The vapour density is determined as follows

$$\rho_v = \frac{\omega*(p_a - p_v)}{87*T} \quad (23)$$

The vapour pressure (p_v) for the air inlet and outlet is calculated with equation 7

$$\dot{Q}_{Hl} = \frac{h_{cm}}{Le^{2/3} C_{p,a}} L(\omega_c - \omega_a) \quad (24)$$

The heat transfer coefficient of biomass humidifier under forced air flow rate presented in Ndukwu et al., [40]as follows

$$h_{cm} = 1.453 \times 10^5 u - 3.03 \times 10^3 T_{db} - 3.985 \times 10^4 u^2 + 77.56 T_{db}^2 + 3.422 \times 10^3 u^3 - 5.88 \times 10^{-1} T_{db}^3 + 3.44 \times 10^2 u T_{db} - 6.398 u T_{db}^2 + 8.207 u^2 T_{db} - 1.48 \times 10^5$$

$R^2 = 0.932$ (25)

2.3 Other performance indices

Temperature – humidity index (THI)

The THI estimates the heat stress effect in evaporative cooling [41]. It's a function of ambient dry bulb and wet bulb temperature estimated empirically for DEC systems as follows

$$THI = 0.6T_{db} + 0.4T_{wb} \quad (26)$$

Specific water consumption

This is the mass of evaporated water per unit area of exposed wetting pad and temperature given as follows [38]

$$C_w = \frac{m_e}{A_H(T_{db} - T_c)} \quad (27)$$

Wet bulb efficiency

The wet bulb efficiency is given as follows [39]

$$\eta = \frac{T_a - T_{out}}{T_a - T_{wb}} \quad (28)$$

Enlargement Coefficient

This is an index that evaluates the performance of the humidifier pores with condensation. It is given as follows [4]

$$\xi = \frac{Q_H}{Q_{Hs}} \quad (29)$$

3. Materials and Methods

3.1 Pilot Direct Evaporative Cooler (DEC) Configuration

The pilot evaporative cooler (Fig. 2) used for the experiment is a standalone outdoor direct evaporative cooler (DEC) designed and developed for pre-cooling fruits and vegetables. It is fabricated at the Agricultural Engineering workshop of the Department of Agricultural Engineering, the Federal University of Technology Akure, South West Nigeria. The DEC consists of a hexagonal cold room (0.24 m^3) equipped with three shelves, as shown in Fig. 2, for pre-cooling fruits or vegetables. The hexagonal room is fitted on a steel frame for rigidity. A 20-litre polycarbonate water tank is placed on top of the pre-cooling room and connected to a perforated PVC pipes (2.5 cm diameter) water spray header (10cm^3/s) to deliver water to the top edges of the wetting pad. The water tank has a cover but can be left open for passive cooling. A sump is placed directly under the wetting pad (0.03 m thickness) and linked to a draining tank and recirculation pump (0.075 kW) through a PVC host. The draining tank is equipped with a floater, which automatically activates the water pump when filled to half capacity. The outdoor air supply to the pad is assisted by three axial fans, while a suction fan is placed behind the wetting pad to draw the air into the cold room.

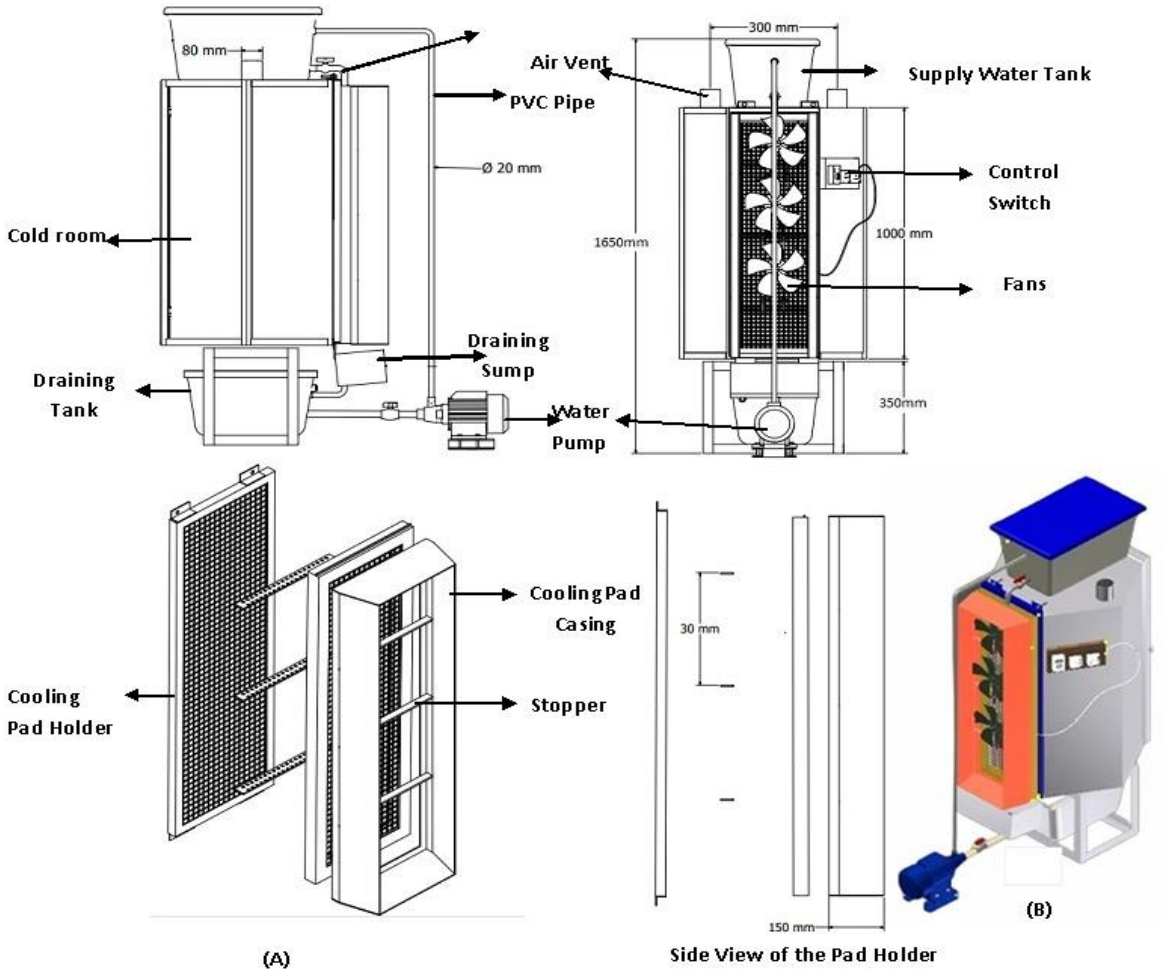

Fig. 2. (A) Orthographic view of the prototyped evaporative cooler showing the front and side elevation of the major components (B) Isometric diagram of the prototyped developed evaporative cooling system

3.2 Preparation and loading of pad materials

Three biomass materials were used as wetting pads and low-cost alternative wetting pads to replace costly imported pads. The pads produce the environment for air humidification in the evaporative cooling process. Each material was obtained locally as a waste product from the end users of the primary sources from cooking, oil milling and bagged product sellers. The materials were manually subjected to size reduction to fit into the evaporative cooling pad holder. The biomass humidifiers and their properties used are presented in Table 1. The biomass materials were loaded at a thickness of 0.03 m (30mm) inside the pad holder, as shown in Figure 2. The design of the pad holder in Figure 2 is such that it is equipped with stoppers to prevent the sagging of the humidifiers.

Table 1: Biomass humidifiers materials

Humidifier	Mass (kg)	Specific heat capacity (kJ/kg K)
Wood Charcoal	2.8	0.8374
Jute fibres	1.3	1.6
Palm fruit mesocarp fibres	0.98	2.816

3.3 Operation scheme of the Pilot DEC

Figure 3 shows the operation scheme of the pilot DEC. The inlet water is delivered at the edges of the wetting pad and stuffed into the pad holder. The water is absorbed by the pad through gravity and capillary action. When the pad is saturated, free water will be available at the pad surface with the absorbed water. This free and absorbed water can supply the needed water for evaporation until the pump re-supplies water again. Upon saturation of the pad, the water discharges into a sump tank directly under the pad. The water percolates and is re-circulated back to the tank with the help of a water pump, and the circle continues. The water pump is activated if the percolating water reaches half of the sump tank. With this, the water pump run time could be controlled. Therefore the pump is not required to work continuously to conserve energy. The outdoor air is supplied to the wet pad with the help of the fan. Due to the water concentration difference, the inlet air is humidified, thus lowering the temperature due to latent heat transfer. With the help of the suction fan, this cold and humidified air are drawn into the cold room, where the stored product is pre-cooled and exits through the vent. The airflow rate is controlled through the fan speed with the help of a rheostat.

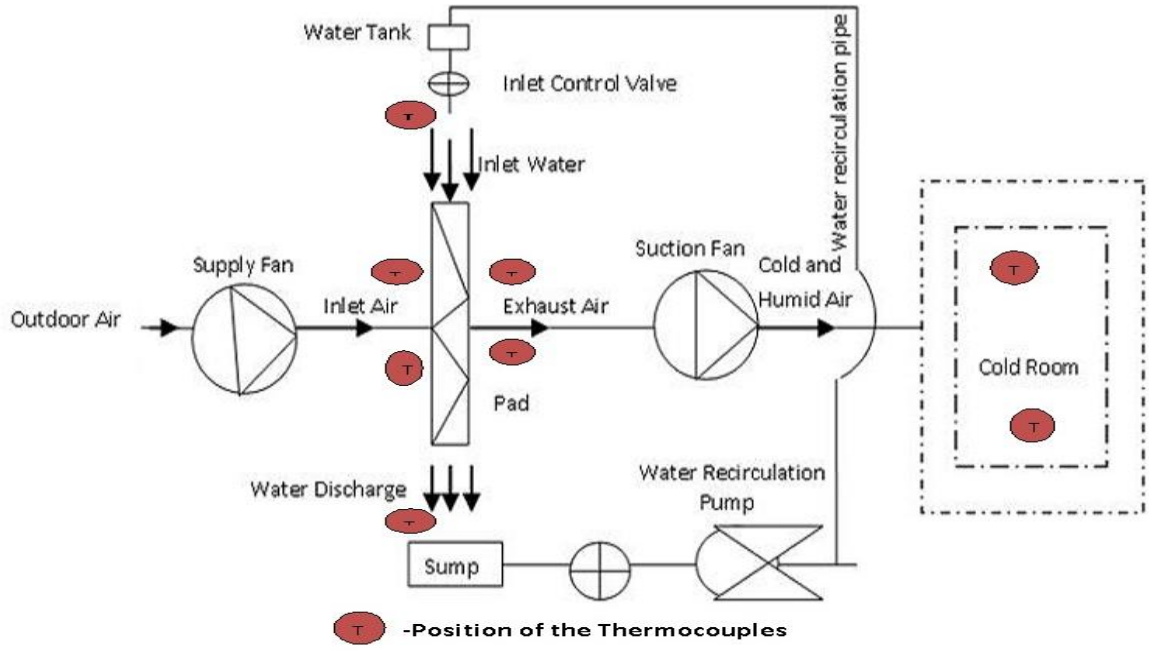

Figure 3: Operational scheme of the pilot DEC

3.4 Field measurement

The experiment was carried out in February to test the capability of the DEC to deliver cold air to the hexagonal room in a tropical environment. The aim is to investigate how fluctuations in various external heat fluxes will affect cold air delivery at variable external conditions of the environment through the humidifier. The DEC was kept outside under an open shade to reduce the direct effect of solar heat and expose the water storage tank of the DEC to wind flow. The 20L water storage tank was left open to allow for passive cooling of the water delivered to the humidifiers through the action of wind which drives the air flux around the tank. Three air flow rates, 4.5, 4.0 and 3.0 m/s, were used to study the transient response of the DEC to external heat flux. This range of air velocity has been used in literature to study the transient response of airflow rates for different DEC pads [25, 42 -43]. After loading the humidifier into the pad holders the water header is opened to deliver water to the edges of the humidifiers. The humidifier was allowed to be thoroughly wetted before switching on the suction fans. The cooler was allowed to stabilize for 1 hr before the non-load reading was logged. Instrumentations used for data collection and their sensitivities are presented in Table 2. The typical ambient condition of the study area in February (Akure Ondo State South West Nigeria) is shown in Table 3.

Table 2: Specifications and sensitivities of measuring instruments

Instruments	Specifications	Sensitivity	Manufacturer
Data logger	HH1147	±0.1^{o}C and ±1 %	Omega Stanford USA
Thermocouple	K-type, USB linked	±0. 1 ◦C	Omega Stanford USA
pyranometer	Apogee MP-200, serial 1250,	±1 W/m^2	APOGEE USA
Digital balance	KERRO model	±0.01 g	KERRO, China
Temperature and humidity clock	DTH-82	±0.1 ^{o}C, ±1.0 %	TLX, Guandong China
Vane anemometer	AM-4826	±2% of the velocity	Landesk, Guangzhou, China

Table 3: Typical Local weather data in February 2013 (Ondo, NG Weather in February) (tcktcktck.org)

Time	Temperature	Dew Point	Humidity	Wind Speed	Pressure	Precipitation
February	° C | ° F	° C | ° F	%	Kph | Mph	Hg | Mb	Total (mm/in)
01	31 | 87.8	6 | 42.8	27	5 | 3.11	29.85 | 1011	0.0 | 0.0
02	31 | 87.8	7 | 44.6	29	5 | 3.11	29.83 | 1010	0.0 | 0.0
03	32 | 89.6	11 | 51.8	36	4 | 2.49	29.8 | 1009	0.0 | 0.0
04	33 | 91.4	15 | 59.0	47	3 | 1.86	29.8 | 1009	0.0 | 0.0
05	34 | 93.2	20 | 68.0	59	4 | 2.49	29.8 | 1009	0.0 | 0.0
06	32 | 89.6	22 | 71.6	70	5 | 3.11	29.83 | 1010	0.8 | 0.03
07	34 | 93.2	20 | 68.0	59	3 | 1.86	29.77 | 1008	0.0 | 0.0
08	35 | 95.0	20 | 68.0	58	4 | 2.49	29.77 | 1008	0.1 | 0.0
09	34 | 93.2	22 | 71.6	64	5 | 3.11	29.74 | 1007	0.3 | 0.01
10	31 | 87.8	22 | 71.6	70	7 | 4.35	29.77 | 1008	1.0 | 0.04
11	31 | 87.8	22 | 71.6	70	6 | 3.73	29.77 | 1008	1.8 | 0.07
12	30 | 86.0	23 | 73.4	76	7 | 4.35	29.77 | 1008	1.1 | 0.04
13	31 | 87.8	23 | 73.4	74	6 | 3.73	29.77 | 1008	2.1 | 0.08
14	31 | 87.8	22 | 71.6	72	7 | 4.35	29.77 | 1008	1.2 | 0.05
15	32 | 89.6	22 | 71.6	72	6 | 3.73	29.77 | 1008	1.5 | 0.06
16	33 | 91.4	21 | 69.8	67	6 | 3.73	29.77 | 1008	4.1 | 0.16
17	30 | 86.0	24 | 75.2	79	7 | 4.35	29.8 | 1009	14.9 | 0.59
18	31 | 87.8	23 | 73.4	75	6 | 3.73	29.77 | 1008	1.1 | 0.04
19	29 | 84.2	23 | 73.4	78	6 | 3.73	29.8 | 1009	7.8 | 0.31
20	30 | 86.0	23 | 73.4	78	6 | 3.73	29.83 | 1010	7.0 | 0.28
21	31 | 87.8	23 | 73.4	76	5 | 3.11	29.8 | 1009	4.2 | 0.17
22	31 | 87.8	23 | 73.4	75	6 | 3.73	29.74 | 1007	2.0 | 0.08
23	31 | 87.8	24 | 75.2	77	5 | 3.11	29.74 | 1007	4.2 | 0.17
24	31 | 87.8	23 | 73.4	76	7 | 4.35	29.74 | 1007	3.4 | 0.13
25	30 | 86.0	23 | 73.4	77	7 | 4.35	29.77 | 1008	1.2 | 0.05

26	31 | 87.8	24 | 75.2	77	7 | 4.35	29.8 | 1009	3.0 | 0.12
27	31 | 87.8	24 | 75.2	78	6 | 3.73	29.8 | 1009	7.9 | 0.31
28	31 | 87.8	24 | 75.2	78	7 | 4.35	29.8 | 1009	8.5 | 0.33

4. Result and Discussion

4.1 Dynamic inlet water temperature response to wind and heat flux variation

In evaporative cooling, the inlet water temperature can directly or indirectly affect the overall performance of evaporative cooling [44]. The design of the evaluated DEC is such that the water tank is exposed to the ambient wind under the shade. The design is on-purpose to expose the water storage tank to air circulation using wind to replace the fan to reduce cost and prevent direct solar radiation heat on the water. It is the utmost belief that the water used in evaporative cooling comes from the underground tap, and there is a tendency for the water temperature to differ depending on the location, depth of pipes and other environmental conditions [45]. However, when the water is used in a standalone evaporative cooler based on the design, there is this tendency for the water to be stored in the tank and reused through a re-circulating pump mechanism. The advantage is that less consumption of water is needed. Still, the stored water tends to accumulate heat before returning to the cooling pad [46]. Therefore, exposing the tank to the wind is one of the ways to cool the water before re-circulation.

However, the heat fluxes/ cooling capacity of air around the storage tank affects the temperature of the tank, and it is also a function of other environmental conditions. Figure 3 presents the relationships between the total heat flux (Q_{total}) on the stored water, cooling water temperature (T_{water}), ambient relative humidity (Rh), ambient temperature (T_{db}) and variation in wind speed. The figure showed that the total heat flux has an inverse relationship with ambient relative humidity and water temperature but has an increasing trend with the wind speed. Due to the passive situation around the water tank, the wind moves away the moist air, which is replaced with dry air, thus reducing the relative humidity and enhancing evaporation [11]. Therefore, the high heat transfer coefficient (h_c) at higher wind or airspeed is compensated by a high evaporation rate [47]. Thus, when the total heat flux increases, the water temperature decreases due to a higher heat exchange rate between the cold, moist air and the drier air because of the decrease in the air's relative humidity and increases in wind speed [38] as shown in Figure 3. This observation has been corroborated by Rehman et al. [47]. They observed that passively cooled systems respond positively to an increase in wind speed. The figure illustrated that the temperature drop between the ambient and water temperature was higher at higher heat flux and wind speed. A higher heat transfer rate to heat air will reduce the cooling load. According to Ahmed et al [46], a lower cooling load will reduce the water flowing through the cooling pads, affecting the exhaust temperature. This agrees with the work of Sellam et al [44], that higher cooling capacity will lead to increased thermal yield. This illustrates the importance of installing a cooling fan around the storage tank of a standalone DEC or choosing a site where the wind speed is high to install the DEC to reduce the cost of chilling the inlet water for DEC systems. This is important because lowering the stored water temperature by increasing the heat flux around the storage tank will provide a higher cooling efficiency for the inlet air into the cooling pad due to lower inlet water temperature. The reason is that the dry bulb inlet temperature will remain the same as the same wet bulb temperature when it comes in contact with inlet water temperature therefore, more heat will be extracted from the air.

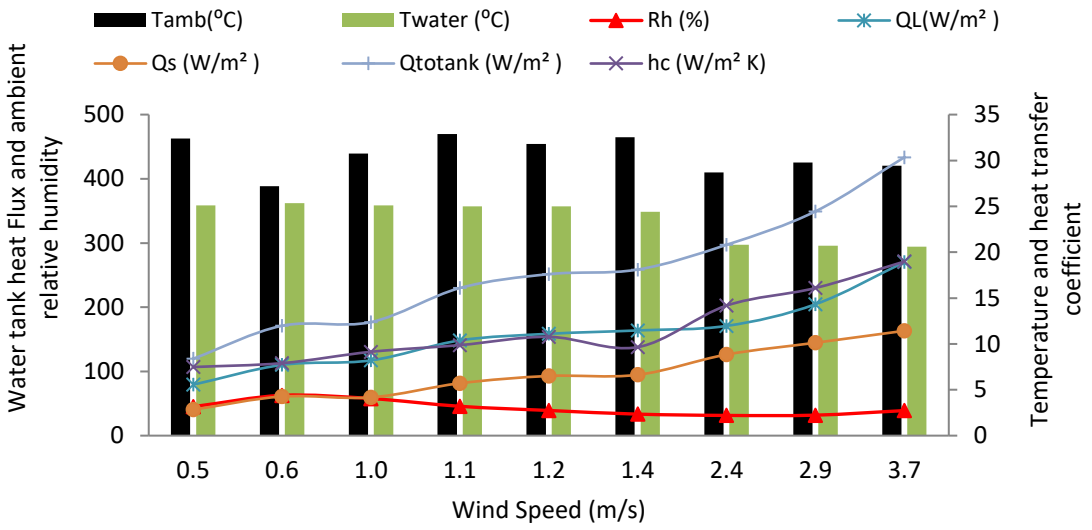

Figure 3: Dynamic response of wind speed to ambient thermodynamic fluxes and water temperature

4.2 Pad exhausts temperature response to variation of inlet water temperature and pad heat flux

To study how this variation in heat flux on water stored in the tank viz-a-viz the inlet water temperature affects the performance of the pad exhaust temperature for the DEC. Three different cooling pads made up of jute fibre, palm fruit mesocarp fibre and wood charcoal were studied independently under active cooling at three air flow rates of 3, 4 and 4.5 m/s. The pad heat flux was calculated separately from the total heat flux on the water tank. It was deduced as a function of pad parameters (pad area, pad thickness etc.), effective thermal conductive of the pad materials (which depends on the humidity difference and degree of saturation) and air flow rate rather than wind speed. The results of average total heat flux (Q_{Htotal}) and pad exhaust temperature (T_c) are presented in figure 4-6 for jute, palm fruit fibres and wood charcoal, respectively. Though the dynamics of the total thermal flux had a clearly defined effect on the water inlet temperature due to the impact of wind on the heat transfer coefficients, its effects on the exhaust temperature were not regular for all the pads. While the heat flux increased with the airflow rate in the jute fibber cooling pad, it decreased for wood charcoal and reached a peak value of 4 m/s for palm fruits mesocarp. However, it was observed that the ambient relative humidity (Rh) of the inlet air and the water temperature had clearly defined effects on the pad exhaust temperature for all the pads and the airflow rate tested. The lower the ambient relative humidity of the inlet air and water temperature, the lower the pad exhaust temperature for the pads and air speeds. This is because, at lower relative humidity, the air has a lower partial water vapour pressure which gives a higher partial pressure gradient resulting in the evaporation of more water resulting in a drop in temperature [48]. Though research has shown that the air flow rate through the pad can play a major role in the degree of air saturation in DEC, however in this case, the air flux through the pad is a combination of the ambient wind flow and the fan-driven air flow rate due to the DEC exposure to the wind. Thus in the case of jute fibre as shown in figure 4 the DEC, temperature (T_c) decreased from 24.44 °C to 24.29°C when the air flow rate increased from 3 m/s to 4 m/s. However, when the airspeed is increased to 4.5 m/s the DEC temperature increases to 24.63°C despite the lower humidity compared to the airflow rate of 3 m/s. Thus as reported by Franco et al [38], as airspeed increased beyond the critical limit at the same pad area, the contact duration between the inlet air to the

pad decreased, resulting in less air moisture saturation, lower saturation efficiency and higher DEC temperature. The performance of DEC depends on the even distribution of water within the cooling pad. Therefore the lesser the contact made by the air with moisture, the lower the performance, irrespective of how low the humidity of inlet air. Nevertheless, the trend for palm fruit mesocarp fibre was different, as shown in figure 5. In figure 5, the pad exhaust temperature decreased with increased air velocity partly due to a decrease in air humidity and water temperature rather than air velocity. This can be confirmed in Figure 6 for wood charcoal, where the pad exhaust temperature decreased with a decrease in water temperature and relative humidity rather than air flow rate. Thus moving air with high relative humidity with high water vapour content will have a lower water retention capacity which will not favour the heat transfer rate [44]. This showed that increasing the heat flux around the water tank and decreasing the relative humidity of the inlet air through the pad will lower the exhaust temperature of the cooling pads. However, Rehman et al. [47] have observed that the degree of the effects of airflow rate on the performance of DEC is localized and dependent on location. In the case of Mali, according to them, going beyond 3 m/s wind speed sets up a diminishing return on performance. Generally, the pad exhaust temperature was lower than the inlet water temperature in all pad materials used. This is the active air flow rate's effect, which quickens the pad materials' evaporation rate. Moreover, the water tank receives residual heat from the shade too. For all the pad materials, the water temperature ranged from 20 .39 to 26.11 ^{o}C, while the pad exhaust temperature ranged from 20.16 to 25.61^{o}C.

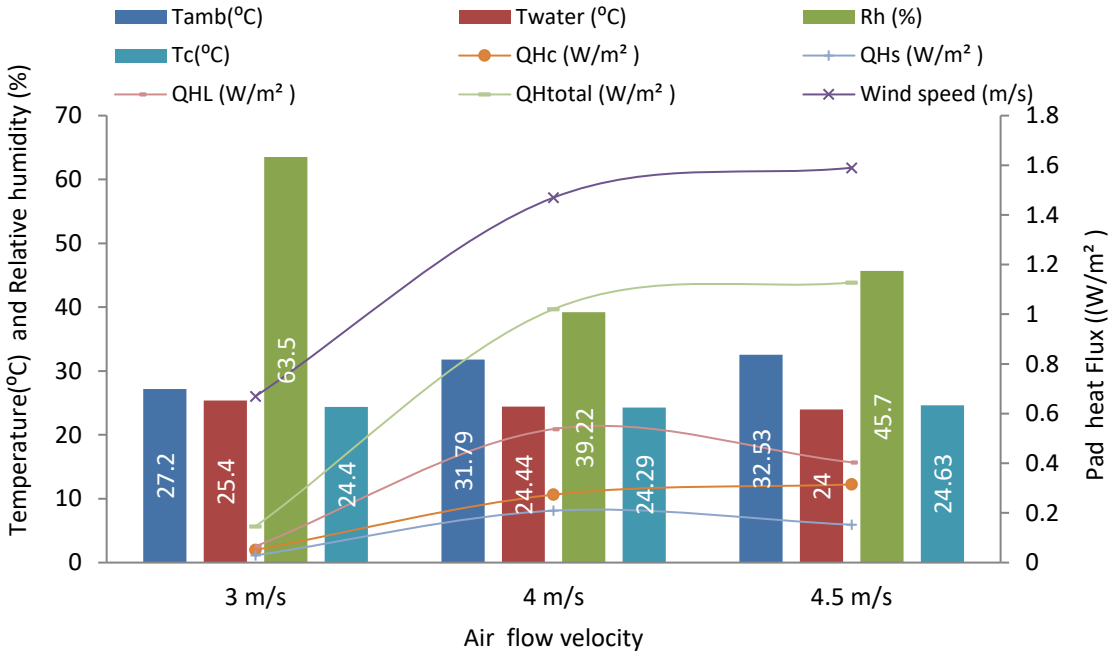

Figure 4: The dynamics of thermal response at different air flow rates for Jute Fiber pad

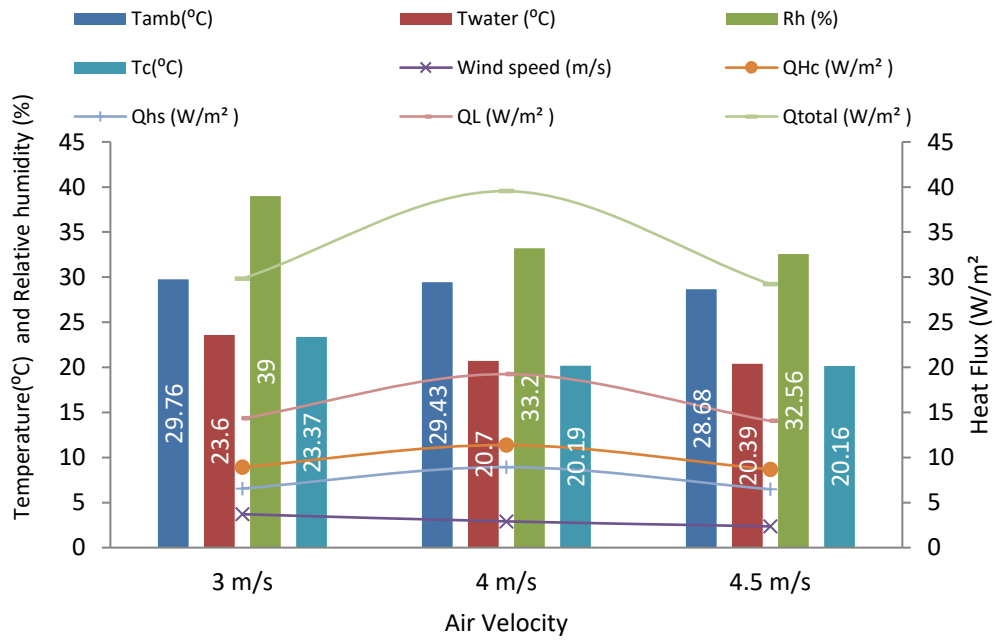

Figure 5: The dynamics of thermal response at different air flow rates for palm fruit mesocarp fibre pad

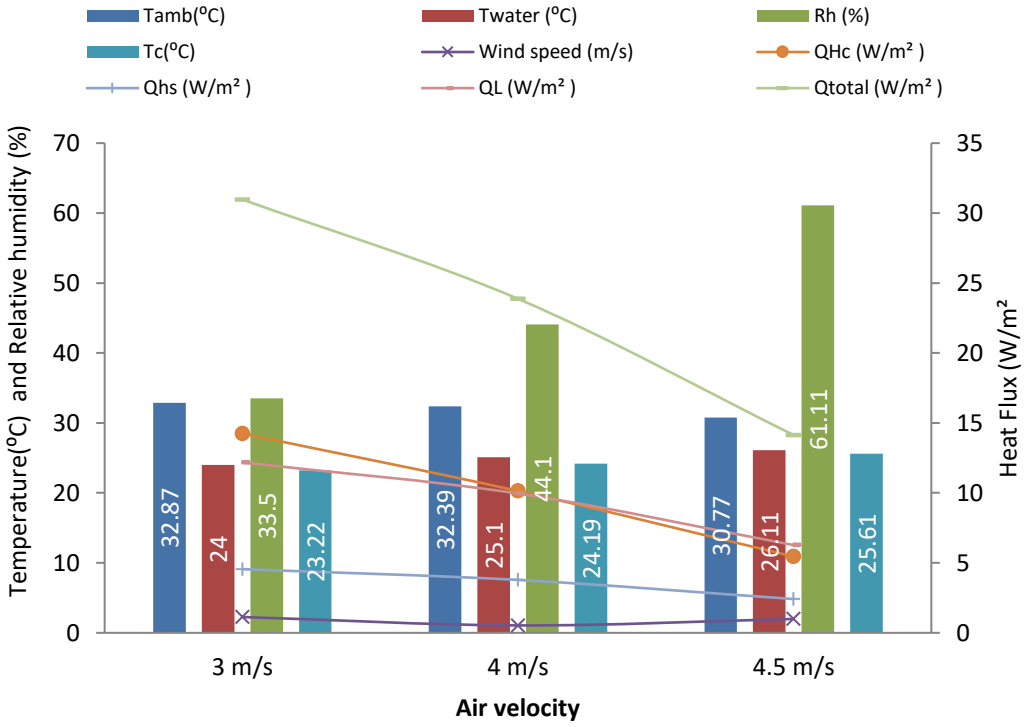

Figure 6: The dynamics of thermal response at different air flow rates for wood charcoal pad

4.3 Thermal –hydraulic performance assessments of the DEC pads

The presented DEC was designed for pre-cooling fruits and vegetables. The output environmental condition requires high humidity and lower temperature to keep the fruits and vegetables fresh. Therefore, the pad thickness, water flow rate and the volume of water delivered to the pad for all the cycle performances were kept constant throughout the experiment. Six performance indices at three different air speeds (3, 4 and 4.5 m/s) were used to evaluate the performances of the three selected biomass pads under similar external environmental conditions of tropical West Africa. The indices were the evaporative efficiency, the specific mass of evaporated water, the temperature-humidity index, the enlargement coefficient, the humidity difference (ΔRh) of the air and the pad exhaust temperature. The thermodynamic properties of air used to deduce the indices are presented in Table 4 for the three pads.

Table 4: Air properties

Pad material	3m/s				4m/s				4.5 m/s			
	h_m	r	r_c	λ_e	h_m	r	r_c	λ_e	h_m	r	r_c	λ_e
Jute	0.4021	0.0008	0.0139	0.0700	0.9777	0.0024	0.0145	0.1306	0.6981	0.0026	0.0140	0.1427
Palm fruit mesocarp	1.1442	0.0019	0.0125	0.1387	1.2809	0.0021	0.0115	0.1540	1.1278	0.0017	0.0111	0.1405
Wood Charcoal	0.5837	0.0026	0.0134	0.1818	0.6267	0.0021	0.0146	0.1585	0.5741	0.0014	0.0162	0.1274

The results of the performance indices are presented in Figures 7-9 for jute fibre, palm fruit mesocarp and wood charcoal, respectively. The airflow rate increased the humidity difference of the exhaust air for palm fruit fibres and wood charcoal pads. In contrast, in the case of jute fibre, it increased from 3 m/s to 4 m/s but decreased at a 4.5 m/s air flow rate. However, this might result from the mass exchange process due to the internal structure of jute fibre. Vapour transfer during evaporative cooling causes an uptick in exhaust air humidity [25]. This vapour transfer depends on the pad material and inlet air properties. Higher air flow rate results in higher separation of moisture molecules leading to free moisture transfer into the cold room where the air inside absorbs this moisture, and the humidity rises. Another reason that can lead to humidity increase of exhaust air is that at a high airflow rate, there is a drop in partial pressure of the inlet air, which creates a higher partial pressure difference between the water–air mass concentration leading to moisture transfer to the air. Thus, the humidity difference between the inlet and exhaust air ranged from 9.94 to 38.7%, with jute fibre having the highest value at 4 m/s while the least humidity difference was obtained at 3 m/s for wood charcoal. On average, wood charcoal had the lowest moisture humidification at the same air flow rate due to large air spaces, while the highest moisture humidification was achieved with jute fibres. At this different range of humidification, the exhaust air humidity ranged from 57.7 % to 91.04 %. This value is good for keeping vegetables fresh at the exhaust temperature range of 20.19 to 25.61^{o}C presented by the cooler performance for the three-speed ranges tested.

Specific water consumption (C_w)is the water evaporated ratio per the wetting pad material unit surface and temperature difference. Figures 7-9 showed that the specific water consumption increased

with airspeed. Higher air flow rate results in higher separation of moisture molecules leading to free moisture transfer. This will leads to a drop in partial pressure of the inlet air, which creates a higher partial pressure difference between the water – air mass concentration resulting in a higher rate of moisture transfer to the air. Therefore, the specific water consumption increased, as shown in Figures 7 to 9, with an increase in humidity difference [25]. Therefore, a higher air flow rate will result in more water consumption. For example, at an airflow rate of 3 m/s, the specific water consumption was higher in palm fruit mesocarp fibre, while at 4 and 4.5 m/s, it was high in wood charcoal, and the value ranged from 9.64 x 10^{-4} to 1.46 x 10^{-3} kg/s.

The wet bulb efficiency decreased with an increase in air flow rate and specific water consumption (C_w) for the palm fruit mesocarp fibres and wood charcoal (Figures 7 and 8). A decrease in the evaporative efficiency of DEC systems with airflow rates has been reported in the literature [49]. High air flow rates can lead to reduced contact time of inlet air and wetting water depending on the pad thickness [50]. This happens because of a decrease in both sensible and latent heat transfer rates. However, the wet bulb efficiency for jute fibre increased from 3 m/s to 4m/s before decreasing the airflow rate to 4.5 m/s (Figure 9). In most cases, except for jute fibre at 4 m/s, higher humidity difference or low cold room temperature did not translate to higher wet bulb cooling effectiveness or efficiency. Still, the lower inlet water temperature significantly affected the evaporative effectiveness. This shows the possibility of free moisture transfer into the cold room from the pad materials at increased air flow rates that helped boost the exhaust air's humidity. The average wet bulb efficiency for the three pads in DEC ranged from 56.4 % to 80.96 %, with jute fibre having a peak value of 4 m/s. This value falls in the range of that obtained for wet bulb effectiveness of DEC presented in the literature [51].

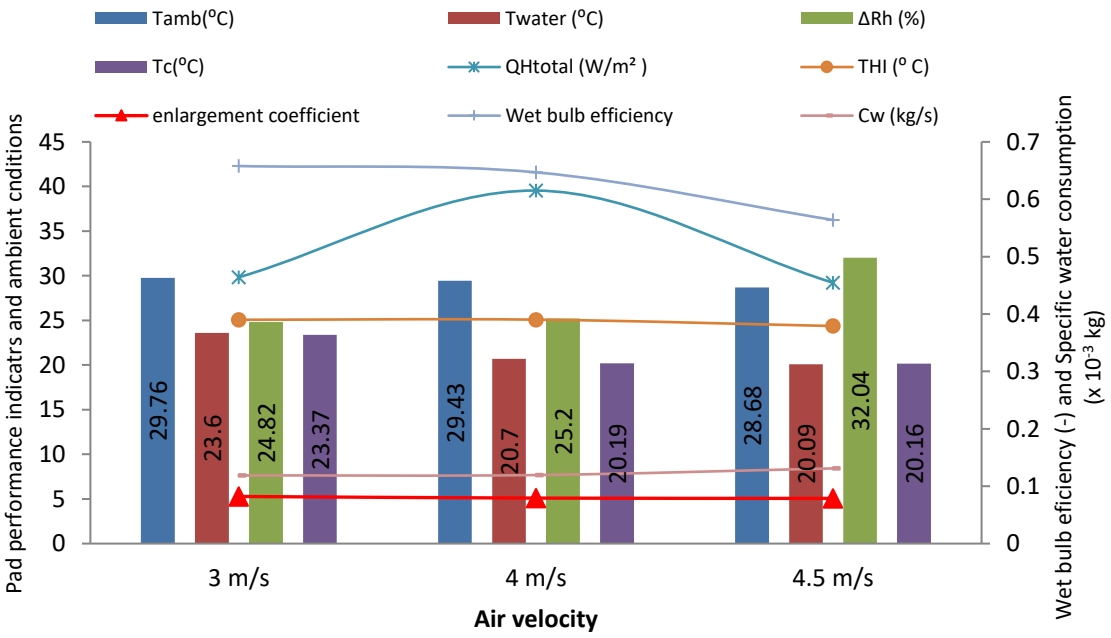

Figure 7: Performance indices for palm fruit mesocarp fibre

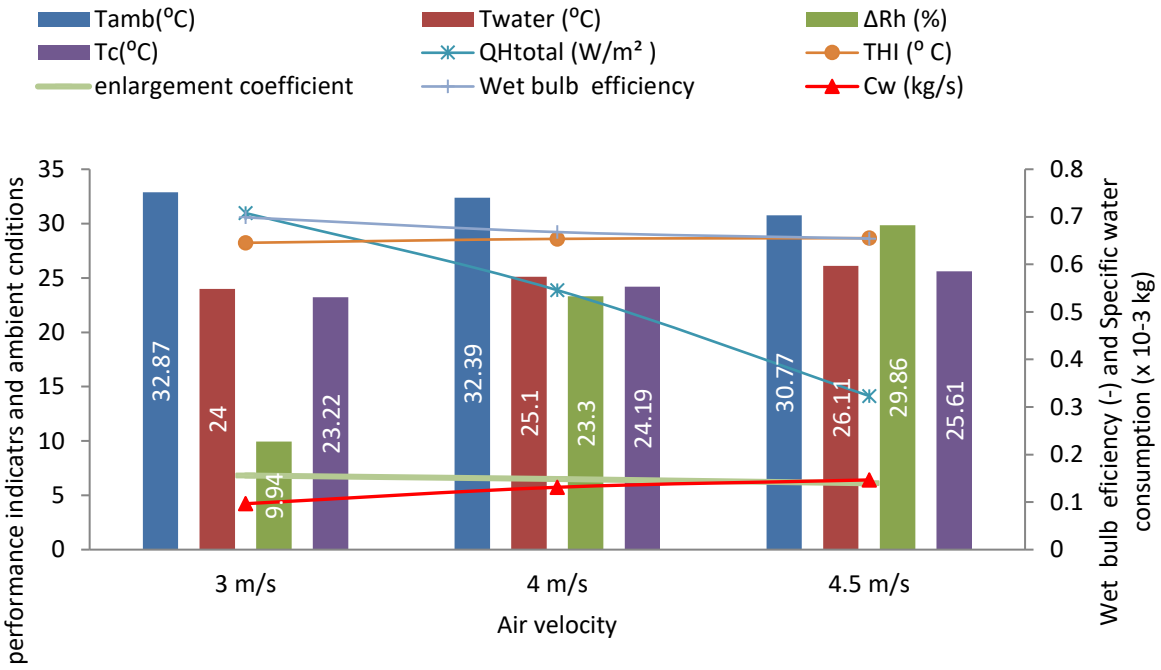

Figure 8: Performance indices for wood charcoal

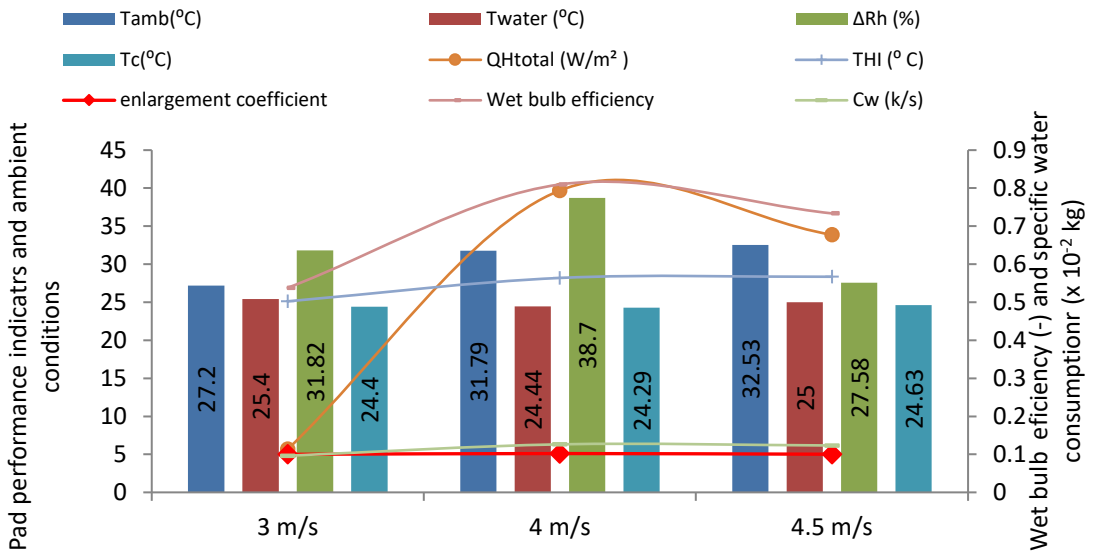

Fig 9: Performance indices for jute fibre

The enlargement coefficient, in this case, is described as the proportion of the total heat transferred to the air, including the latent, radiation and sensible heat to the sensible heat transfer [4]. The enlargement coefficient is influenced by the air condition variation, especially the air humidity. They decrease linearly with the increase in humidity difference and airflow rates. The values for the three pads ranged from 5 to 6.82. However, the values were higher for wood charcoal but lower for jute fibre cooling pads. Temperature stress indicated by the temperature-humidity index was higher in wood charcoal but lower in palm fruits mesocarp. However, they increased with an increase in air flow rate. This observation was

made by Khater [41] using cellulose pads in the Egyptian climate. However, the values ranged from 24.37 to 28.66 ^{o}C.

5.0 Conclusions

The research tries to use theoretical analysis to link the performance of different biomass wetting pads with the inlet water temperature as influenced by the heat flux on the storage tank for DEC systems using the external ambient condition of West sub-Saharan Africa. Although the results showed that increasing the wind flow increases the heat flux on the water tank. However, the ambient relative humidity has a major impact on the inlet water temperature. Therefore, increasing the heat flux around the water tank and decreasing the relative humidity of the inlet air through the pad will lower the exhaust temperature of the cooling pads. Decreasing the inlet water temperature leads to a decrease in the exhaust air temperature of all the wetting pads, while an increased air flow rate reduces the evaporative efficiency. Heat flux behaviour on the wetting pads is erratic; however, increasing the air flow rate increased water consumption for the pads. Six indices were considered in terms of the thermal-hydraulic performances of the pads, including evaporative efficiency, the specific mass of evaporated water, temperature-humidity index, enlargement coefficient, the humidity difference of the air and the pad exhaust temperature at three airflow velocities. The humidity difference of the exhaust air for palm fruits fibres and wood charcoal pads increased with the air flow rate, while in the case of jute fibre, it increased from 3 m/s to 4 m/s but decreased at 4.5 m/s air flow rate. Thus, the humidity difference between the inlet and exhaust air ranged from 9.94 to 38.7%, with jute fibre having the highest value at 4 m/s while the least humidity difference was obtained at 3 m/s for wood charcoal.

At an airflow rate of 3 m/s, the water demand was higher in palm fruit mesocarp fibre, while at 4 and 4.5 m/s it was higher in wood charcoal and the value ranged from 9.64×10^{-4} to 1.46×10^{-3} kg/s. Except for jute fibre at 4 m/s, higher humidity difference or low cold room temperature did not translate to higher evaporative cooling effectiveness or efficiency, but lower inlet water temperature had a greater effect on the evaporative effectiveness. This shows the possibility of free moisture transfer into the cold room from the pad materials at increased air flow rates that helped boost the exhaust air's humidity. The average evaporative efficiency for the three pads in DEC ranged from 56.4 % to 80.96 %, however, jute fibber had the best performance at 4 m/s among the biomass fibbers with the highest average wet-bulb efficiency. The values for the enlargement coefficient for the three pads ranged from 5 to 6.82, while the temperature thermal stress values ranged from 24.37 to 28.66 ^{o}C. The obtained data will be useful in developing evaporative coolers for pre-cooling fruits and vegetables in Sub-Saharan Africa using biomass materials. However, proper and regular monitoring of the pad is needed to avoid microbial growth. Therefore the biomass pads should be changed regularly since they come with little or at no cost. In future research, we will focus on how to treat biomass fibres to achieve long-term durability of the biomass fibbers to extend their useful life in the EVC.

References

1. Mahmood MH, Sultan M, Miyazaki T (2019). Significance of temperature and humidity control for agricultural products storage: an overview of conventional and advanced options. *International Journal of Food Engineering*, 15(10): 20190063.
2. Raza H M.U., M Sultan, M Bahrami , A A. Khan (2020).Experimental investigation of evaporative cooling systems for agricultural storage and livestock air-conditioning in Pakistan. Build Simul https://doi.org/10.1007/s12273-020-0678-2

3. Ndukwu M. C, S. I. Manuwa , L. Bennamoun , O. J. Olukunle, F. I. Abam (2019). In-Situ Evolution of Heat and Mass Transfer Phenomena and Evaporative Water Losses of Three Agro-Waste Evaporative Cooling Pads: An Experimental and Modeling Study. Waste and Biomass Valorization (2019) 10:3185–3195 https://doi.org/10.1007/s12649-018-0315-9
4. Yang, H., Shi, W., Chen, Y., & Min, Y. (2021). Research development of indirect evaporative cooling technology: An updated review. Renewable and Sustainable Energy Reviews, 145(April), 111082. https://doi.org/10.1016/j.rser.2021.111082
5. Pacak, A., & Worek, W. (2021). Review of dew points evaporative cooling technology for air conditioning applications. Applied Sciences (Switzerland), 11(3), 1–16. https://doi.org/10.3390/app11030934
6. Ndukwu M. C., S.I.Manuwa .(2014). Review of research and application of evaporative cooling in the preservation of fresh agricultural produce. Int J Agric & Biol Eng, 2014; 7(5): 85－102
7. Ghani, S., Bakochristou, F., ElBialy, E. M. A. A., Gamaledin, S. M. A., Rashwan, M. M., Abdelhalim, A. M., & Ismail, S. M. (2019). Design challenges of agricultural greenhouses in hot and arid environments – A review. Engineering in Agriculture, Environment and Food, 12, 48–70. https://doi.org/10.1016/j.eaef.2018.09.004
8. Al Assaad, D. K., Orabi, M. S., Ghaddar, N. K., Ghali, K. F., Salam, D. A., Ouahrani, D., Farran, M. T., & Habib, R. R. (2021). A sustainable localised air distribution system for enhancing the thermal environment and indoor air quality of poultry houses for semiarid regions. Biosystems Engineering, 203, 70–92. https://doi.org/10.1016/j.biosystemseng.2021.01.002
9. Hussain, G.; Aleem, M.; Sultan, M.; Sajjad, U.; Ibrahim, S.M.; Shamshiri, R.R.; Farooq, M.; Usman. Khan, M.; Bilal, M. (2022). EvaluatingEvaporative Cooling Assisted Solid Desiccant Dehumidification System for Agricultural Storage Application.Sustainability **2022**, 14, 1479.
10. Ambuko J., F. Wanjiru, G.N. Chemining'wa, W.O. Owino, E. Mwachoni, Preservation of postharvest quality of leafy amaranth (Amaranthus spp.) vegetables using evaporative cooling, J. Food Qual. 2017 (2017) 1–7, DOI: 10.1155/2017/5303156
11. Islam M.P, T. Morimoto (2015). Evaluation of a new heat transfer and evaporative design for a zero energy storage structure. Solar Energy 118, 469–484
12. Ndukwu M.C. (2011). Development of clay evaporative cooler for fruits and vegetable preservation, Agric. Eng. Int. CIGR J. 13 (1) (2011) 1–8 2011.
13. Dadhich, S. M., Dadhich, H., Verma, R. (2008). Comparative Study on Storage of Fruits and Vegetables in Evaporative Cool Chamber and Ambient. International Journal of Food Engineering, *4(1)*. doi:10.2202/1556-3758.1147 10.2202/1556-3758.114
14. Shrivastava K., D. Deshmukh, M.V. Rawlani (2014).Experimental analysis of coconut coir pad evaporative cooler, Int. J. Innov. Res. Sci., Eng. Technol 3, 8346–8351.
15. Rawangkul R., J. Khedari, J. Hirunlabh, B Zeghmati, Performance analysis of a new sustainable evaporative cooling pad made from coconut coir, Int. J. Sustain. Eng. 1 (2) (2008) 117–131
16. Jain J.K., D.A Hindoliya, Experimental performance of new evaporative cooling pad materials, Sustain. Cities Soc. 1 (4) (2011) 252–256, DOI: 10.1016/j.scs.2011.07.005
17. Velasco-Gómez, E., Tejero-González, A., Jorge-Rico, J., & Rey-Martínez, F. J. (2020). Experimental Investigation of the Potential of a New Fabric-Based Evaporative Cooling Pad. Sustainability, 12(17), 7070. doi:10.3390/su12177070
18. Dogramacı P. A, S. Riffat , G. Gan , D.Aydın (2019). Experimental study of the potential of eucalyptus fibres for evaporative cooling, Re- new. Energy 131 250–260.
19. Aziz R.A, N. F.Zamrud, N Rosli (2018). Comparison of cooling efficiency of cooling pad materials for an evaporative cooling system. Journal of modern manufacturing systems and technology 01, 061-068

20. Shekhar R, Chopra MK, Purohit R. Design of a compact evaporative cooler to improve cooling efficiency and to evaluate the performance of different cooling pad material. Int J Sci Res Dev 2016;4:21–7.
21. Ahmed EM, Abaas O, Ahmed M, Ismail MR. (2011) Performance evaluation of three different types of local evaporative cooling pads in greenhouses in Sudan. Saudi J Biol Sci 2011;18:45–51. https://doi.org/10.1016/j.sjbs.2010.09.005
22. Tejero-Gonz_alez, A., & Franco-Salas, A. (2021). Optimal operation of evaporative cooling pads: A review. Renewable and Sustainable Energy Reviews, 151, 111632.
23. ASHRAE (2019). Evaporative cooling. In ASHRAE handbook – HVAC applications.Atlanta, GA:
24. Dai YJ, Sumathy K (2002). Theoretical study on a cross-flow direct evaporative cooler using honeycomb paper as packing material.*Applied Thermal Engineering*, 22: 1417–1430.
25. Nada S.A., H.F. Elattar, M.A. Mahmoud, A. Fouda (2020). Performance enhancement and heat and mass transfer characteristics of direct evaporative building free cooling using corrugated cellulose papers. Energy 211 (2020) 118678
26. Velasco-G_omez, E., Tejero-Gonz_alez, A., Jorge-Rico, J., & Rey-Martínez, F. J. (2020). Experimental investigation of the potential of a new fabric-based evaporative cooling pad. Sustainability (Switzerland), 12(17). https://doi.org/10.3390/su12177070
27. Ketwong, W., Deethayat, T., & Kiatsiriroat, T. (2021). Performance enhancement of air conditioners in hot climates by condenser cooling with cool air generated by direct evaporative cooling. Case Studies in Thermal Engineering, 26(January), 101127. https://doi.org/10.1016/j.csite.2021.101127
28. Chen, W., Liu, S., & Lin, J. (2015). Analysis of the passive evaporative cooling wall constructed of porous ceramic pipes with water-sucking ability. Energy and Buildings, 86, 541–549. https://doi.org/10.1016/j.enbuild.2014.10.055
29. Ndukwu, M. C., & Manuwa, S. I. (2015). A techno-economic assessment for the viability of some waste as cooling pads in an evaporative cooling system. International Journal of Agricultural and Biological Engineering, 8(2), 151–158. https://doi.org/10.3965/j.ijabe.20150802.952\
30. Alamdari, P., Saedodin, S., & Rejvani, M. (2020). Do non-metallic materials and radiation shields affect the operation of direct evaporative cooling systems? International Journal of Refrigeration, 114, 98–105. https://doi.org/10.1016/j.ijrefrig.2020.02.038
31. Tejero-Gonz_alez, A., & Franco-Salas, A. (2021). Direct evaporative cooling from wetted surfaces: Challenges for a clean air conditioning solution. Wiley Interdisciplinary Reviews: Energy and Environment, e423. https://doi.org/10.1002/wene.423
32. Zizak. T, S. Domjan, S. Medved, C. Arkar (2022).Efficiency and sustainability assessment of evaporative cooling of photovoltaics. Energy 254 (2022) 124260
33. Kloppers JC, Kr€oger DG. The Lewis factor and its influence on the performance prediction of wet-cooling towers. Int J Therm Sci 2005;44:879e84. https:/doi.org/10.1016/j.ijthermalsci.2005.03.006.
34. Chengqin, R., & Hongxing, Y. (2006). An analytical model for the heat and mass transfer processes in indirect evaporative cooling with parallel/counter flow configurations. International Journal of Heat and Mass Transfer, 49(3-4), 617–627. doi:10.1016/j.ijheatmasstransfer.2005.08.019.0
35. Nugent A, David DeCou, Shintaro Russell, and Christina Karamperidou (2019). Atmospheric Processes and Phenomenon. Atmospheric science. ATMO 200 texts. Outreach college university of Hawaii at manoa oer.hawaii.ed. Chapter 4: Water Vapor – Atmospheric Processes and Phenomenon (hawaii.edu)

36. Slavinec M, R. Repnik, E. Klemenčič (2016).The impact of moisture on the thermal conductivity of fabrics. ANALI PAZU, 6/ 2016/1-2, str. 8-12
37. Stull R.(2011), Wet-bulb temperature from relative humidity and air temperature, Journal of applied meteorology and climatology 50 (2011) 22672269.
38. Franco, D. L. Valera, A. Madueno, A. Pena (2010) Influence Of Water And Air Flow On The Performance Of Cellulose Evaporative Cooling Pads Used In Mediterranean Greenhouses. Transactions of the ASABE: Vol. 53(2): 565-576
39. Ndukwu M.C., M.I. Ibeh, E.C. Ugwu, D.O. Igbojionu, A.A. Ahiakwo, Hongwei Wu (2022). Evaluating coefficient of performance and rate of moisture loss of some biomass humidifier materials with a developed simple direct standalone evaporative cooling system for farmers. Energy Nexus 8 (2022) 100146
40. Ndukwu C, S. Manuwa, O. Olukunle, B.Oluwalana (2013). A simple model for evaporative cooling space in a tropical climate. Agricultura Engineering (3), 27 – 39
41. Khater ESG (2014) Performance of Direct Evaporative Cooling System under Egyptian Conditions. J Climatol Weather Forecasting 2:119. doi:10.4172/2332-2594.1000119
42. Dhamneya, S. P.S. Rajput, A. Singh, Thermodynamic performance analysis of a direct evaporative cooling system for increased heat and mass transfer area, Ain Shams Eng. J. 9 (4) (2018) 2951–2960, https://doi.org/10.1016/j. asej.2017.09.008.
43. Doˇgramacı P.A., S. Riffat, G. Gan, D. Aydın, Experimental study of the potential of eucalyptus fibres for evaporative cooling, Renew. Energy 131 (2019) 250–260, https://doi.org/10.1016/j.renene.2018.07.005. A.K.
44. Sellam S, A.Moummi, C. Mehdid, A. Rouag, A. Benmachiche , M. Melhegueg, A. Benchabane (2022). Experimental performance evaluation of date palm fibres for a direct evaporative cooler operating in the hot and arid climate. Case Studies in Thermal Engineering 35 (2022) 102119
45. Sheng C, A.G. Agwu Nnanna (2012). Empirical correlation of cooling efficiency and transport phenomena of direct evaporative cooler. Applied Thermal Engineering 40 (2012) 48-55
46. Ahmed F., F. Shaik, Waqar Ahmed Khan et al (2021). Experimental assessment of multi-purpose evaporative type cooler used for refrigeration and air cooling, Materials Today: Proceedings, https://doi.org/10.1016/j.matpr.2021.07.129
47. Rehman D, E. McGarrigle, L. Glicksman, E Verploegen (2020).A heat and mass transport model of clay pot evaporative coolers for vegetable storage. International Journal of Heat and Mass Transfer 162 (2020) 120270
48. Weichao Yan, Xin Cui, Xiaohu Yang, Liwen Jin, Xiangzhao Meng (2020). Performance evaluation of a direct evaporative cooling system with hollow fibre-based heat exchanger. International Conference on Sustainable Energy and Green Technology 2019 IOP Conf. Series: Earth and Environmental Science **463** (2020) 012023 IOP Publishing doi:10.1088/1755-1315/463/1/012023.
49. Kovacˇevic´ I., M. Sourbron / (2017). The numerical model for direct evaporative coolerApplied Thermal Engineering 113 (2017) 8–19
50. Bishoyi D, K. Sudhakara (2017).Experimental performance of a direct evaporative cooler in a composite climate of India. Energy and Buildings 153 (2017) 190–200
51. Kim Min-Hwi, Jae-Weon Jeong (2013). Cooling performance of a 100% outdoor air system integrated with indirect and direct evaporative coolers. Energy 52 (2013) 245-257